SCIENTIFIC REPORTS

OPEN

SUBJECT AREAS:
FERROELECTRICS AND MULTIFERROICS
FERROMAGNETISM
SURFACES, INTERFACES AND THIN FILMS
ELECTRONIC PROPERTIES AND MATERIALS

Received
7 May 2013

Accepted
22 August 2013

Published
10 September 2013

Correspondence and requests for materials should be addressed to H.Y. (yanghao@suda.edu.cn) or S.J. (jusheng@suda.edu.cn)

Oxygen-Vacancy-Induced Antiferromagnetism to Ferromagnetism Transformation in $Eu_{0.5}Ba_{0.5}TiO_{3-\delta}$ Multiferroic Thin Films

Weiwei Li[1], Run Zhao[1], Le Wang[2], Rujun Tang[1], Yuanyuan Zhu[3], Joo Hwan Lee[3], Haixia Cao[1], Tianyi Cai[1], Haizhong Guo[2], Can Wang[2], Langsheng Ling[4], Li Pi[4], Kuijuan Jin[2], Yuheng Zhang[4], Haiyan Wang[3], Yongqiang Wang[5], Sheng Ju[1] & Hao Yang[1]

[1]Jiangsu Key Laboratory of Thin Films, School of Physical Science and Technology, Soochow University, Suzhou 215006, China, [2]Beijing National Laboratory for Condensed Matter Physics and Institute of Physics, Chinese Academy of Science, Beijing 100190, China, [3]Materials Science and Engineering Program, Department of Electrical and Computer Engineering, Texas A&M University, College Station, Texas 77843-3128, USA, [4]High Magnetic Field Laboratory, Chinese Academy of Science, Hefei 230031, China, [5]Materials Science and Technology Division, Los Alamos National Laboratory, Los Alamos, New Mexico 87545, USA.

Oxygen vacancies (V_O) effects on magnetic ordering in $Eu_{0.5}Ba_{0.5}TiO_{3-\delta}$ ($EBTO_{3-\delta}$) thin films have been investigated using a combination of experimental measurements and first-principles density-functional calculations. Two kinds of $EBTO_{3-\delta}$ thin films with different oxygen deficiency have been fabricated. A nuclear resonance backscattering spectrometry technique has been used to quantitatively measure contents of the V_O. $Eu_{0.5}Ba_{0.5}TiO_3$ ceramics have been known to exhibit ferroelectric (FE) and G-type antiferromagnetic (AFM) properties. While, a ferromagnetic (FM) behavior with a Curie temperature of 1.85 K has been found in the $EBTO_{3-\delta}$ thin films. Spin-polarized Ti^{3+} ions, which originated from the V_O, has been proven to mediate a FM coupling between the local Eu 4*f* spins and were believed to be responsible for the great change of the magnetic ordering. Considering the easy formation of V_O, our work opens up a new avenue for achieving co-existence of FM and FE orders in oxide materials.

Multiferroics, or materials that simultaneously possess two or more ferroic orders [ferroelectric, (anti-) ferromagnetic, and ferroelastic], have recently returned to the forefront of materials research due to their rich physical properties and potential applications in data storage, sensors, and spintronics[1,2]. From an application point of view, multiferroics with ferromagnetic-ferroelectric (FM-FE) orders are more attractive and highly desired[3]. However, very few exist in nature due to the intrinsic contradiction in existence between the FM and FE ordering within a single phase[4]. On the other hand, antiferromagnetic-ferroelectric (AFM-FE) materials are more commonly found, such as rare-earth manganites ($RMnO_3$) and the well known $BiFeO_3$[5–11]. It is fundamentally interesting and technologically important to develop FM-FE materials by changing magnetic ordering of the AFM-FE materials. An additional driving force and a deep understanding of physical phenomenon underlying the transformation are needed to realize this purpose.

In oxides, oxygen vacancies (V_O) have been approved to be intrinsic defects and are believed to have a critical impact on their properties[12]. Coey *et al* reported that V_O play a key role in obtaining room temperature FM in HfO_2, ZnO, TiO_2, and other non-magnetic oxide systems[13–16]. It has also been proven that V_O are useful in increasing Curie temperature and enhancing magnetic moment of EuO thin films[17–20]. Furthermore, V_O are known to induce a room temperature ferroelectricity in $SrTiO_3$ thin films[21–23]. Despite the fact that the V_O are effective to manipulating the magnetic and ferroelectric properties of oxides, little attention has been focused upon the V_O effects on multiferroicity in single-phase materials. A natural question to ask is: are the V_O able to change the magnetic ordering from AFM to FM in multiferroic materials?

The beginning of the present work is to choose a suitable material to verify the above idea. In recent years, divalent europium oxidation materials showed attractive functionalities, rendering them subjects of intensive studies. Compared to the 0.05 μ_B/Fe in $BiFeO_3$[24], rare-earth Eu^{2+} ion has seven unpaired and localized 4*f* electrons, which resulted in a large magnetization of 7 μ_B/Eu and sometimes is coupled with electrical properties.

For example, Rushchanskii *et al* confirmed that $Eu_{0.5}Ba_{0.5}TiO_3$ (EBTO) ceramics exhibit FE (Curie temperature $T_C \sim 213$ K) and G-type AFM (Néer temperature $T_N \sim 1.9$ K) properties[25]. And coupling between magnetism and dielectric properties was predicted in $Eu_{1-x}Ba_xTiO_3$ materials[26]. Furthermore, as we discussed earlier, the V_O have been proven to be useful in manipulating the magnetic orders of divalent Eu ions in EuO thin films. Therefore, EBTO is a potential material for the present study, based on the nature of a large magnetization of 7 μ_B/Eu and the AFM-FE orders. In addition, if we can alter magnetism of EBTO thin films by doping V_O and at the same time still preserve good ferroelectricity, it will certainly make EBTO itself appealing in fundamental research and practical applications. In the present work, we experimentally confirmed that the magnetic ordering in oxygen-deficient $Eu_{0.5}Ba_{0.5}TiO_{3-\delta}$ ($EBTO_{3-\delta}$) thin films has been transformed from AFM to FM. First-principle calculations indicated that spin-polarized Ti^{3+} ions, which originated from the V_O, mediated a FM coupling between the local Eu 4*f* spins. Considering the easy formation of V_O, our work presented an effective technique to achieve co-existence of FM and FE orders in oxide materials.

Results

The $EBTO_{3-\delta}$ thin films were fabricated on (001) oriented $SrTiO_3$ (STO) and Nb-doped $SrTiO_3$ (Nb-STO) substrates by pulsed laser deposition (PLD). Following the deposition, parts of the thin films were post-annealed under a reducing atmosphere to increase amount of the V_O. Typical X-ray diffraction (XRD) θ–2θ scans confirmed that the $EBTO_{3-\delta}$ is preferentially oriented along the *c* axis (not shown). In order to reveal the microstructure of the $EBTO_{3-\delta}$ thin films, cross-sectional transmission electron microcopy (TEM) measurements were conducted. A low magnification bright-field TEM image (Fig. 1a) shows that the interface is clean without any obvious interface reaction or intermixing. In the view area, the film is continuous without any obvious grain boundaries, confirming the 2D growth of the film. The corresponding selected area diffraction (SAD) image taken from the interface area is shown as inset of Fig. 1a. The distinguished diffraction dots from the film and substrate indicate the high quality epitaxial growth. The out-of-plane and in-plane orientation relationships have been determined to be $(001)_{EBTO}||(001)_{STO}$ and $[110]_{EBTO}||[110]_{STO}$, respectively. A high resolution TEM (HRTEM) image (Fig. 1b) confirmed the excellent heteroepitaxial relation with an atomically sharp interface. Similarly no obvious misfit dislocations have been found along the interface, which is consistent with the SAD observation.

To quantitatively analyze stoichiometry and oxygen concentration of the $EBTO_{3-\delta}$ thin films, a nuclear resonance backscattering spectrometry (NRBS) technique was used. The advantage of NRBS over traditional Rutherford backscattering spectrometry (RBS) is its sensitivity to selectively measure oxygen in the $EBTO_{3-\delta}$ film on an oxygen-rich substrate, such as STO in our experiment[27,28]. The NRBS was performed using a 3.043 MeV $^4He^+$ analyzing beam and the backscattering particles were detected by a surface barrier silicon detector located at 167° from the beam direction. At such a beam energy, the He scattering from the heavier elements (Eu, Ba, and Ti) in the film is still Rutherford, therefore the Eu:Ba:Ti ratios

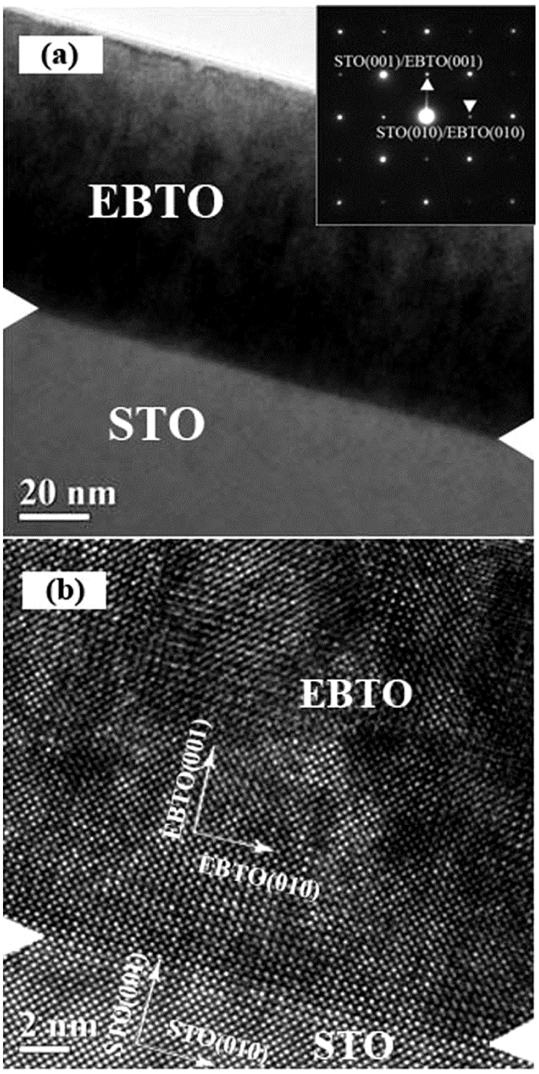

Figure 1 | TEM images of the $EBTO_{3-\delta}$ thin film on a STO substrate: (a) low magnification cross-sectional TEM; (b) high resolution TEM (HRTEM). The inset shows the corresponding selected-area diffraction (SAD) pattern.

can be determined reasonably well by fitting the experimental spectra data with the commercial Rutherford Universal Manipulation Program (RUMP) software[29]. Within the uncertainty of the measurements (~5%), we determined that our $EBTO_{3-\delta}$ thin films do have an Eu:Ba:Ti ratio of 1 : 1 : 2.

After the atomic ratios of cations were determined, a nuclear scattering and reaction simulation package (SIMNRA) was used to fit the nuclear resonant oxygen scattering spectra (not shown)[30]. To minimize uncertainties related to the nuclear scattering cross section and the incident beam energy, a bare STO substrate as a standard reference was measured and analyzed all together along with our

Table 1 | The measured concentration of europium and oxygen from the NRBS. The content of V_O (x), the value of δ (δ = 3×), and the ideal and real content of Ti^{3+} are also shown. The ideal content of Ti^{3+} is estimated from δ with a relationship of Ti^{3+}/Ti:δ = 2 : 1. The real values are calculated by fitting peaks of XPS measurements

			Oxygen vacancies			
	Eu(at./cm^2)	O(at./cm^2)	x	δ	Ideal Ti^{3+}/Ti	Real Ti^{3+}/Ti
As-deposited thin film	8.7×10^{16}	5.01×10^{17}	4.0%	0.120	24.0%	27.1%
Annealed thin film	9.8×10^{16}	5.58×10^{17}	5.1%	0.153	30.6%	33.4%

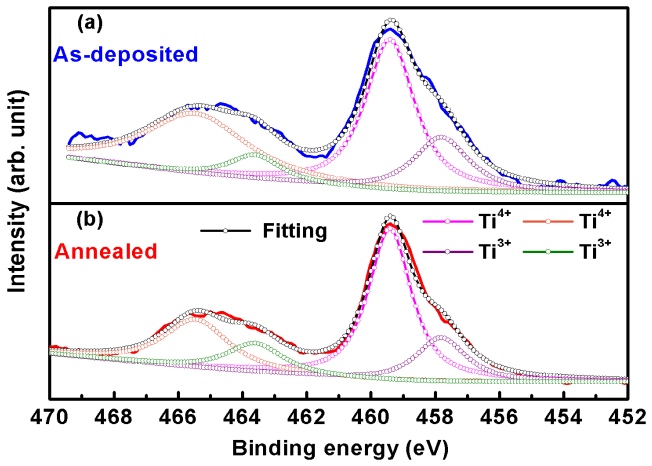

Figure 2 | The open circles represent peak fittings on these graphs, which show the Ti 2*p* core-level photoemission spectra of (a) as-deposited and (b) annealed $EBTO_{3-\delta}$ thin films.

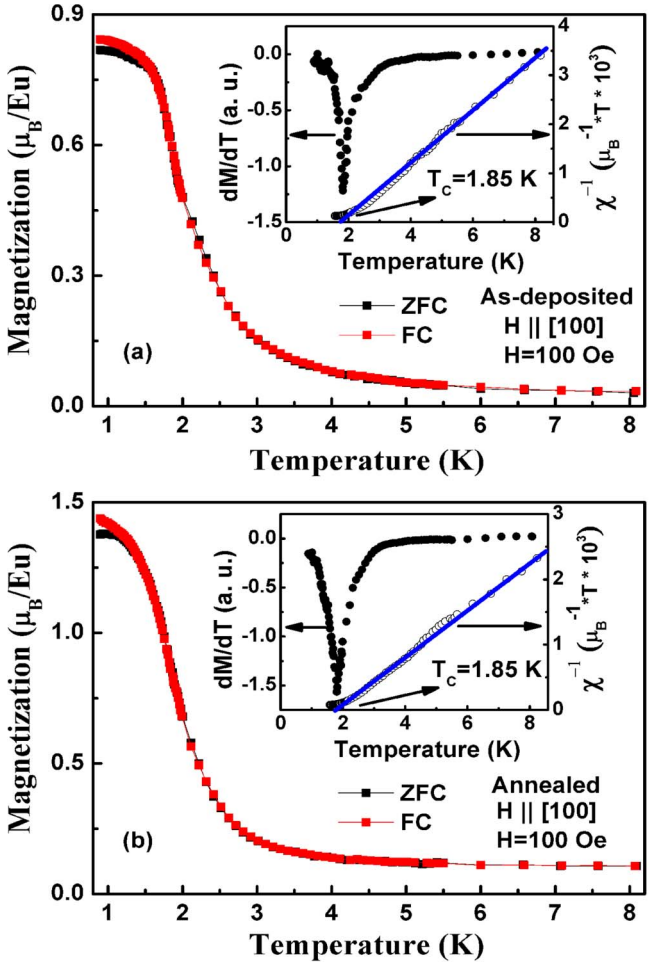

Figure 3 | Temperature dependence of magnetization curves under ZFC and FC conditions for the (a) as-deposited and (b) annealed $EBTO_{3-\delta}$ films. The insets show the derivative of the magnetization (the solid circles) and the reciprocal susceptibility (the open circles) with respect to the temperature (obtained from the FC curves). The blue lines on the insets are the Curie-Weiss law fittings of the reciprocal susceptibilities.

$EBTO_{3-\delta}$ thin films. Table 1 shows the measured concentration of europium and oxygen in the as-deposited and annealed $EBTO_{3-\delta}$ thin films. From the Eu concentration, the ideal oxygen concentration in the stoichiometric $Eu_{0.5}Ba_{0.5}TiO_3$ thin films is estimated to be 5.22×10^{17} and 5.88×10^{17} at./cm^2 for as-deposited and annealed thin films respectively. By comparing the measured and the ideal oxygen concentration, we have calculated that there are 4.0% oxygen deficiency ($\delta \approx 0.120$) in the as-deposited film and 5.1% oxygen deficiency ($\delta \approx 0.153$) in the annealed film. In other words, the V_O were introduced into the $EBTO_{3-\delta}$ thin films and the content of the V_O were increased by post-annealing under a reducing atmosphere.

Because of the charge compensation, the existence of V_O should induce changes in the valance states of cations. To quantify these changes, we investigated the valance states of the $EBTO_{3-\delta}$ thin films by using X-ray photoemission spectroscopy (XPS). We found that the valence states of Eu and Ba ions are remained in divalent (not shown), while those of Ti ions have been changed. Because V_O act as *n*-type dopants, the Ti^{3+} and Ti^{4+} formal valences should coexist in the $EBTO_{3-\delta}$ thin films. Figure 2 shows Ti 2*p* core-level photoemission spectrum of (a) the as-deposited and (b) the annealed $EBTO_{3-\delta}$ thin films with peak fittings. Compared with previous results, the peaks at a binding energy around 459.42 eV and 465.45 eV can be assigned as Ti^{4+}, with peaks around 457.81 eV and 463.53 eV corresponding to Ti^{3+} [31,32]. By comparing the peak area, the content of Ti^{3+} was calculated to be 27.1% and 33.4% in the as-deposited and annealed thin films respectively. On the other hand, by assuming two free carries for each V_O[33], the ratio between the content of Ti^{3+} and that of V_O (δ) will be 2 : 1. Therefore, the ideal content of Ti^{3+} for the

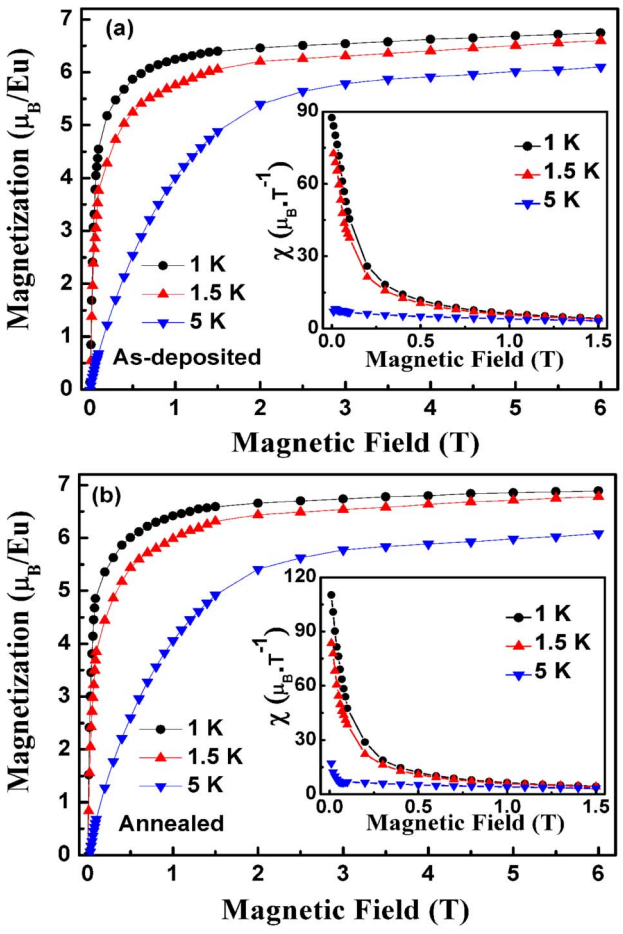

Figure 4 | Magnetic field dependent magnetization curves for (a) as-deposited and (b) annealed $EBTO_{3-\delta}$ thin films at various temperature. The insets show magnetic susceptibility curves.

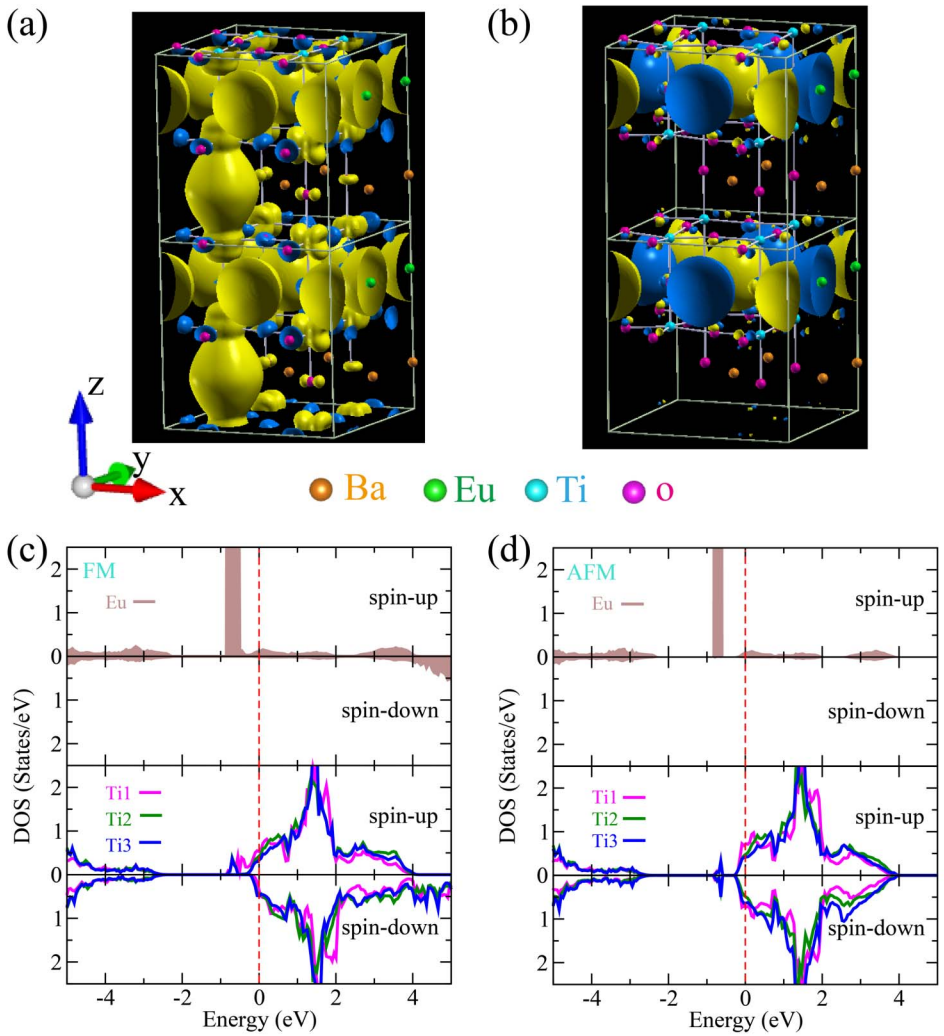

Figure 5 | Spin-density and local density of states (DOS) in the $EBTO_{3-1/8}$: (a) and (c) for FM ground state; (b) and (d) for AFM state. Here, yellow color is for up-spin and blue color for down-spin. The red vertical dash line is the Fermi level. Ti1, Ti2, and Ti3 are the nearest (just below the V_O), next-nearest (at the same *ab*-plane of Ti1), and next-next-nearest (at the same *ab*-plane of Ti1) Ti ions with respect to the V_O. The Eu ions are almost similar to each other. The development of spin-polarized d_{z^2} orbital at Ti^{3+} is obvious in the FM ground state.

as-deposited and annealed thin films should be 24.0% and 30.6% respectively (see table 1). These results are well fitted with the calculated values and further confirmed that V_O were doped into the thin films. In addition, the fact that the change of the valence states only occurred in Ti cations has been verified by first-principles density-functional calculations and will be discussed in more details later.

To investigate V_O effects on magnetic properties of the $EBTO_{3-\delta}$ thin films, temperature and magnetic-field dependences of magnetization were investigated using a superconducting quantum interface device magnetometer (SQUID). Figure 3 shows the temperature dependent magnetization curves. The measurements were performed under zero-field-cooled (ZFC) and field-cooled (FC) conditions with an external magnetic field of 100 Oe applied parallel to the films surface. The EBTO ceramics antiferromagnetically ordered at 1.9 K[25]. However, the magnetization on both ZFC and FC curves increased monotonically with decreasing temperature until 0.9 K and tend to be saturated at the lowest temperature, which is a typical FM behavior. The derivative of the magnetization and the reciprocal susceptibility as a function of temperature are shown as insets of Fig. 3a and 3b. It has been found that the derivative of the magnetization shows a sharp valley, in other words the magnetizations increase quickly, at around 1.85 K. In addition, the Curie-Weiss law fitting of the reciprocal susceptibilities at high temperatures intersects the temperature axis at 1.85 K. Both of these results then confirmed the FM ordering in the $EBTO_{3-\delta}$ thin films with a Curie temperature of 1.85 K[34]. Figure 4 shows the field dependent magnetization curves at 1, 1.5, and 5 K. It has been found that, at 1 and 1.5 K, the magnetization increased sharply at low fields and then approached saturation quickly. The large susceptibility at low fields (shown as insets of Fig. 4a and 4b) is also an evidence for the FM ordering below 1.85 K. The saturation magnetizations, measured for the as-deposited and annealed thin films at 1 K, are around 6.75 μ_B/Eu and 6.85 μ_B/Eu respectively. These values are close to the ideal magnetic moment of the Eu^{2+} ions (7 μ_B/Eu). It should be noticed that the susceptibility at low fields and the value of the magnetization in the annealed thin films are larger than those in the as-deposited thin films, which obviously originates from the enhanced content of V_O. In order to further prove the FM ordering of the $EBTO_{3-\delta}$ thin films below 1.85 K, magnetic hysteresis loops were measured at 0.5 K (Supplementary Figure S1). Hysteretic behavior is observed with a coercivity of 30 Oe. The combination of these results proved that the $EBTO_{3-\delta}$ thin films become a ferromagnet with a Curie temperature of 1.85 K, which is different from bulk EBTO – G-type antiferromagnet[25].

Many theoretical studies of vacancy-induced magnetism in non-magnetic $SrTiO_3$ have been performed using ab initio

Table 2 | Energy differences between AFM and FM states in $EBTO_{3-1/4}$ with various atomic orderings of Eu and Ba ions. In all the cases, FM state is energetically favorable. In addition, A-type atomic arrangement of Eu and Ba ions is the ground state

	A-type atomic ordering	C-type atomic ordering	G-type atomic ordering
ΔE = E(AFM) − E(FM) (meV/Eu)	0.6	0.2	0.5

calculations[35,36]. To investigate the fundamental physics underlying the origin of the FM ordering in the $EBTO_{3-\delta}$ thin films, we calculated total energies of $EBTO_{3-1/8}$ with both FM and AFM orderings from first-principles density-functional theory. FM ordering is found to be 13.1 meV/Eu favorable. Figure 5 shows the spin-density and local density of states (DOS) in the $EBTO_{3-1/8}$: (a) and (c) for FM ground state; (b) and (d) for AFM state. As shown in DOS of local Ti ions, the occupancy of 3*d* orbital indicates the appearance of Ti^{3+}, in good agreement with the XPS measurements. Furthermore, the existence of V_O does not change the valence state of Eu, since almost fully occupied $4f^7$ states are found, which is similar to the pristine $EuTiO_3$ and confirmed by the SQUID and XPS measurements[37]. On the other hand, as shown in Fig. 5 (a) and (c), the development of large local spin moment at Ti sites makes the FM ground state differ significantly from the AFM state. The local magnetic moment at Ti^{3+} ions right above or under V_O is around 0.24 μ_B and the d_{z^2} dominates. While for other Ti^{3+} ions, the local orbital is either d_{xy} or d_{xz}/d_{yz}. Magnetic moment at Eu site does not change from the pristine case with a local magnetic moment of around 7 μ_B. Judging from Fig. 5, it is the appearance of spin-polarized Ti^{3+} that mediates the FM coupling between the localized Eu 4*f* spins. It should be noticed that with increase of the content of V_O, e.g. $Eu_{0.5}Ba_{0.5}TiO_{3-1/4}$, the FM ordering is still found to be energetically favorable than the AFM orderings (see Table 2). These results verified that the $EBTO_{3-\delta}$ thin films do show FM ordering, which originated from the ordering of the spin of Eu 4*f* electrons mediated by the spin-polarized Ti^{3+} ions.

This article is mainly concerned about the magnetic ordering, but we also investigated the FE properties of the annealed $EBTO_{3-\delta}$ thin films by measuring dielectric constant as a function of temperature and room-temperature hysteresis loop using piezoresponse force microscopy (PFM). It's surprised to find out that a peak in dielectric constant versus temperature curves (shown as Fig. 6) is clearly seen above room temperature. Moreover, a room-temperature hysteresis loop measured by PFM was shown as inset of Fig. 6. These results suggest that the FE Curie temperature of the annealed $EBTO_{3-\delta}$ thin films is above room temperature, which is significantly higher than that of bulk EBTO (~213 K). The investigation on mechanism of the enhancement on the FE Curie temperature is presently in progress.

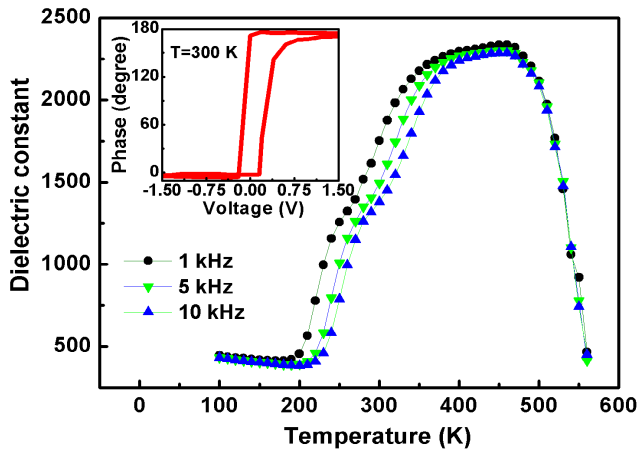

Figure 6 | Temperature dependence of dielectric constant for the annealed $EBTO_{3-\delta}$ thin film. The inset shows room-temperature hysteresis loop measured by PFM.

Discussion

In summary, two kinds of $EBTO_{3-\delta}$ thin films with different content of V_O were fabricated. By using NRBS, SQUID, and first-principles calculations, we demonstrated that the magnetic ordering of oxygen-deficient $EBTO_{3-\delta}$ thin films has been changed from AFM to FM. The transformation originated from the V_O induced Ti 3*d* electrons, which mediated the FM coupling between the local Eu 4*f* spins. The results are significant as they proved that V_O are effective to manipulating magnetic ordering in multiferroic materials. Considering the easy formation of V_O, the present work presents a methodology to enhance multiferroicity in the $EBTO_{3-\delta}$ thin films and this method holds great promise for other oxide materials.

Methods

The $EBTO_{3-\delta}$ thin films were fabricated on (001) oriented $SrTiO_3$ (STO) and Nb-doped $SrTiO_3$ (Nb-STO) substrates by pulsed laser deposition (PLD) using a pulsed excimer laser (Lambda Physik, 248 nm, 3 Hz, 2 J/cm^2). A high-density EBTO ceramic pellet was used as the target. The details of the preparation of EBTO ceramics can be found in elsewhere[25]. Deposition temperature was 700°C and oxygen pressure was 1×10^{-4} Pa with the purpose of doping V_O. Following the deposition, parts of the thin films were annealed at 1000°C under a flowing gas of 95 vol% Ar + 5 vol% H_2 for 10 hours to increase amount of the V_O. The film thickness, revealed by cross-sectional transmission electron microcopy (TEM), was 100–150 nm.

The crystal structures were characterized by X-ray diffraction (XRD, Rigaku K/Max) and TEM (FEI Tecnai F20 analytical microscope). Nuclear resonance backscattering spectrometry (NRBS) was performed on Los Alamos National Laboratory. A He^+ beam energy of 3.043 MeV was used to quantitatively analyze stoichiometry and oxygen concentration in the $EBTO_{3-\delta}$ thin films. The valence states were investigated by X-ray photoemission spectroscopy (XPS) at PHI5000 VersaProbe.

Magnetic measurements were performed on $EBTO_{3-\delta}$/STO thin films using a superconducting quantum interface device magnetometer (SQUID) equipped with a He^3 insert (Quantum Design, MPMS-XL). The electrical properties were measured using a Pt/$EBTO_{3-\delta}$/Nb-STO heterostructure. The dielectric constants were investigated using an Agilent 4294A Impedence Analyzer. The measurements were performed at selected temperatures in a Linkam Scientific Instruments HFS600E-PB4 system. Room-temperature piezoresponse force microscopy (PFM) was measured using PFM mode of Asylum Research MFP-3D-SA atomic force microcopy.

Our ab initio calculations are performed using the accurate full-potential projector-augmented wave (PAW) method, as implemented in the Vienna ab initio simulation package (VASP)[38,39]. They are based on density-functional theory with the generalized gradient approximation (GGA) in the form proposed by Perdew, Burke, and Ernzerhof (PBE)[40]. The on-site Coulomb interaction is included in the GGA + U approach with effective U = 4 eV for Eu 4*f* orbitals[41]. A plane-wave cutoff of 600 eV is used throughout and the convergence criteria for energy is 10^{-6} eV. PAW potentials are used to describe the electron-ion interaction with 17 valence electrons for Eu ($4f^7 5s^2 5p^6 6s^2$), 10 for Ba ($5s^2 5p^6 6s^2$), 10 for Ti ($3p^6 3d^2 4s^2$), and 6 for O ($2s^2 2p^4$). In our calculations, ions are relaxed toward equilibrium positions until the Hellman-Feynman forces are less than 1 meV/A. In addition, lattice constants are optimized until the stress is less than 0.001 Pa. The fully optimized lattice constant of $Eu_{0.5}Ba_{0.5}TiO_3$ stems from an initial cubic lattice, from which the atoms shift a little from their high symmetric positions. Total energies are calculated and compared between different magnetic and A-site atomic arrangements.

1. Eerenstein, W., Mathur, N. D. & Scott, J. F. Multiferroic and magnetoelectric materials. *Nature* **442**, 759–765 (2006).
2. Ramesh, R. & Spaldin, N. A. Multiferroics: progress and prospects in thin films. *Nat. Mater.* **6**, 21–29 (2007).
3. Spaldin, N. A., Cheong, S. W. & Ramesh, R. Multiferroics: Past, present, and future. *Phys. Today* **63**, 38–43 (2010).
4. Hill, N. A. Why are there so few magnetic ferroelectrics. *J. Phys. Chem. B* **104**, 6694–6709 (2000).
5. Kimura, T. *et al.* Magnetic control of ferroelectric polarization. *Nature* **426**, 55–58 (2003).
6. Kimura, T., Lawes, G., Goto, T., Tokura, Y. & Ramirez, A. P. Magnetoelectric phase diagrams of orthorhombic $RMnO_3$ (R = Gd, Tb, & Dy). *Phys. Rev. B* **71**, 224425 (2005).
7. Fujimura, N., Ishida, T., Yoshimura, T. & Ito, T. Epitaxially grown $YMnO_3$ film: New candidate for nonvolatile memory devices. *Appl. Phys. Lett.* **69**, 1011 (1996).

8. Yakel, H. L., Koehler, W. C., Bertaut, E. F. & Forrat, E. F. On the crystal structure of the manganese(III) trioxides of the heavy lanthanides and yttrium. *Acta Cryst.* **16**, 957–962 (1963).
9. Bertaut, E. F., Pauthenet, R. & Mercier, M. Properties magnetiques et structure du manganite d'yttrium. *Phys. Lett.* **7**, 110–111 (1963).
10. Kiselev, S. V., Ozerov, R. P. & Zhdanov, G. S. Detection of magnetic order in ferroelectric $BiFeO_3$ by neutron diffraction. *Sov. Phys. Dokl.* **7**, 742–744 (1963).
11. Teague, J. R., Gerson, R. & James, W. J. Dielectric hysteresis in single crystal $BiFeO_3$. *Solid State Commun.* **8**, 1073–1074 (1970).
12. Yang, H. *et al.* Vertical interface effect on the physical properties of self-assembled nanocomposite epitaxial films. *Adv. Mater.* **21**, 3794–3798 (2009).
13. Venkatesan, M., Fitzgerald, C. B. & Coey, J. M. D. Thin films: Unexpected magnetism in a dielectric oxide. *Nature* **430**, 630 (2004).
14. Coey, J. M. D., Venkatesan, M. & Fitzgerald, C. B. Donor impurity band exchange in dilute ferromagnetic oxides. *Nat. Mater.* **4**, 173–179 (2005).
15. Ramachandran, S., Naryan, J. & Prater, J. T. Effect of oxygen annealing on Mn doped ZnO diluted magnetic semiconductors. *Appl. Phys. Lett.* **88**, 242503 (2006).
16. Philip, J. *et al.* Carrier-controlled ferromagnetism in transparent oxides semiconductors. *Nat. Mater.* **5**, 298–304 (2006).
17. Matsumoto, T. *et al.* Preparation of Gd-doped EuO_{1-x} thin films and the magnetic and magneto-transport properties. *J. Phys. Condens. Matter* **16**, 6017 (2004).
18. Wang, X. *et al.* Effects of Gd doping and oxygen vacancies on the properties of EuO films prepared via pulsed laser deposition. *IEEE Tran. Magn.* **46**, 1879–1882 (2010).
19. Liu, P., Tang, J., Colón Santana, J., Belashchenko, K. D. & Dowben, P. Ce-doped EuO: Magnetic properties and the indirect band gap. *J. Appl. Phys.* **109**, 07C311 (2011).
20. Barbagallo, M. *et al.* Experimental and theoretical analysis of magnetic moment enhancement in oxygen-deficient EuO. *Phys. Rev. B.* **81**, 235216 (2010).
21. Kim, Y. S. *et al.* Localized electronic states induced by defects and possible origin of ferroelectricity in strontium titanate thin films. *Appl. Phys. Lett.* **94**, 202906 (2009).
22. Choi, M., Oba, F. & Tanaka, I. Role of Ti antisitelike defects in $SrTiO_3$. *Phys. Rev. Lett.* **103**, 185502 (2009).
23. Jang, H. W. *et al.* Ferroelectricity in strained-free $SrTiO_3$ thin films. *Phys. Rev. Lett.* **104**, 197601 (2010).
24. Ederer, C. & Spaldin, N. A. Weak ferromagnetism and magnetoelectric coupling in bismuth ferrite. *Phys. Rev. B* **71**, 060401 (2005).
25. Rushchanskii, K. Z. *et al.* A multiferroic material to search for the permanent electric dipole moment of the electron. *Nat. Mater.* **9**, 649–654 (2010).
26. Wu, H., Jiang, Q. & Shen, W. Z. Coupling between the magnetism and dielectric properties in $Eu_{1-x}Ba_xTiO_3$. *Phys. Rev. B* **69**, 014104 (2004).
27. Gibson, G. T., Wang, Y. Q., Sheu, W. J. & Glass, G. A. Oxygen depth profiling by nuclear resonant scattering. *AIP Conf. Proc.* **475**, 549–553 (1999).
28. Yang, H., Wang, Y. Q., Wang, H. & Jia, Q. X. Oxygen concentration and its effect on the leakage current in $BiFeO_3$ thin films. *Appl. Phys. Lett.* **96**, 012909 (2010).
29. Doolittle, L. R. Algorithms for the rapid simulation of Rutherford backscattering spectra. *Nuclear Instruments and Methods in Physics Research B* **9**, 344–351 (1985).
30. Mayer, M. SIMNRA, a simulation program for the analysis of NRA, RBS, and ERDA. *AIP Conf. Proc.* **475**, 541–544 (1999).
31. Pertosa, P. & Michel-Calendini, F. M. X-ray photoelectron spectra, theoretical band structures, and densities of states for $BaTiO_3$ and $KNbO_3$. *Phys. Rev. B* **17**, 2011–2020 (1978).
32. Nasser, S. A. X-ray photoelectron spectroscopy study on the composition and structure of $BaTiO_3$ thin films deposited on silicon. *Appl. Surf. Sci.* **157**, 14–22 (2000).
33. Muller, D. A., Nakagawa, N., Ohtomo, A., Grazul, J. L. & Hwang, H. Y. Atomic-scale imaging of nanoengineered oxygen vacancy profiles in $SrTiO_3$. *Nature* **430**, 657–661 (2004).
34. Chikazumi, S. *Physics of ferromagnetism.* 118–148 (Clarendon Press, Oxford, 1997).
35. Shein, I. R. & Ivanovskii, A. L. First principle prediction of vacancy-induced magnetism in non-magnetic perovskite $SrTiO_3$. *Phys. Lett. A* **371**, 155–159 (2007).
36. Zhang, Y. J., Hu, J. F., Cao, E. S., Sun, L. & Qin, H. W. Vacancy induced magnetism in $SrTiO_3$. *J. Magn. Magn. Mater.* **324**, 1770–1775 (2012).
37. Scagnoli, V. *et al.* $EuTiO_3$ magnetic structure studied by neutron powder diffraction and resonant x-ray scattering. *Phys. Rev. B* **86**, 094432 (2012).
38. Blöchl, P. E. Projector augmented-wave method. *Phys. Rev. B* **50**, 17953–17979 (1994).
39. Kresse, G. & Furthmuller, J. Efficiency of ab-initio total energy calculations for metals and semiconductors using a plane-wave basis set. *Comput. Mater. Sci.* **6**, 15–50 (1996).
40. Perdew, J. P., Burke, K. & Ernzerhof, M. Generalized gradient approximation made simple. *Phys. Rev. Lett.* **77**, 3865–3868 (1996).
41. Dudarev, S. L., Botton, G. A., Savrasov, S. Y., Humphreys, C. J. & Sutton, A. P. Electron-energy-loss spectra and the structural stability of nikel oxide: An LSDA + U study. *Phys. Rev. B* **57**, 1505–1509 (1998).

Acknowledgements

The authors acknowledge the support of the National Natural Science Foundation of China (Grant No. 11004145, 11274237, 11134012, 11104193, 51228201, and 51202153), the Natural Science Foundation of Jiangsu Province under Grant No. SBK201021263, the Scientific Research Foundation for the Returned Overseas Chinese Scholars (State Education Ministry of China), and the Priority Academic Program Development of Jiangsu Higher Education Institutions (PAPD). Partial support for thin film characterization was also provided by the Center for Integrated Nanotechnologies, a DOE nanoscience user facility, jointly operated by Los Alamos and Sandia National Laboratories. The TEM work at Texas A&M University is funded by the US National Science Foundation (NSF-0846504).

Author contributions

H.Y. supervised the project. W.L., R.Z. and R.T. conducted the thin films fabrication and data analysis. W.L., L.W., H.G., C.W. and K.J. did the electrical properties measurements. Y.Z., J.H.L. and H.W. helped to collect and analyze the TEM images. L.L., L.P. and Y.Z. conducted the SQUID measurements. Y.W. performed the NRBS measurements. H.C., T.C. and S.J. did the first-principles calculations. W.L., H.Y. and S.J. co-wrote the manuscript. All authors reviewed the manuscript.

Additional information

Supplementary information accompanies this paper at http://www.nature.com/scientificreports

Competing financial interests: The authors declare no competing financial interests.

How to cite this article: Li, W. *et al.* Oxygen-Vacancy-Induced Antiferromagnetism to Ferromagnetism Transformation in $Eu_{0.5}Ba_{0.5}TiO_{3-\delta}$ Multiferroic Thin Films. *Sci. Rep.* **3**, 2618; DOI:10.1038/srep02618 (2013).